

## **DATING SINTER DEPOSITS IN NORTHERN DIXIE VALLEY, NEVADA- THE PALEOSEISMIC RECORD AND IMPLICATIONS FOR THE DIXIE VALLEY GEOTHERMAL SYSTEM**

S. Juch Lutz<sup>1</sup>, S.J. Caskey<sup>2</sup>, D.D. Mildenhall<sup>3</sup>, P.R.L. Browne<sup>4</sup>, and S.D. Johnson<sup>5</sup>

1. Energy & Geoscience Institute, University of Utah, Salt Lake City, UT 84108
2. Department of Geosciences, San Francisco State University, San Francisco, CA 94132
3. Institute of Geological and Nuclear Sciences, Lower Hutt, New Zealand
4. Geothermal Institute and Geology Dept., University of Auckland, Auckland, New Zealand
5. Caithness Operating Corp., Reno, NV 89511  
e-mail: sjlutz@egi.utah.edu

### **ABSTRACT**

A series of fossil spring deposits are exposed along the Dixie Valley fault just south of the producing geothermal field, in an area now characterized by active fumaroles and steaming ground. These deposits are composed of both travertine and sinter that have trapped pollen and other plant material during their formation. Radiocarbon dates on the organic material indicate that the youngest hot spring sinters range in age from about 3.4 ka to essentially modern. Banded travertine composed of calcite, dolomite, hematite, and barite may represent deposition from a warm spring at about 5040 ka. Older quartz-rich sinters are between 3.4 ka and Lake Dixie (11-12 ka) in age.

The mineralogy and texture of the opaline sinters are consistent with their young ages. One sinter (with a modern <sup>14</sup>C age) consists of botryoidal heads of vitreous, opaline silica or "geyserite" that likely formed from actively spouting eruptions of boiling fluids along the fault zone. X-ray diffraction analyses indicate that the sinter is composed of original opal-A that has not undergone the transition to the more crystalline opal-CT or cristobalite (opal-C). Slightly older (2.2 to 3.4 ka) sinters appear to be admixtures of opal-C or opal-CT, microcrystalline quartz, and calcite. These sinters are predominantly thinly laminated to porous opal-CT, and contain abundant plant remains and clasts of even older microcrystalline quartz sinter.

The radiocarbon dates reveal the episodic nature of spring activity along the Dixie Valley fault. Paleoseismic studies identify several large magnitude earthquakes in the central Dixie Valley area that may be related to the spring activity. Two of these seismic events are historic, the 1915 M7.7 Pleasant Valley and the 1954 M6.8 Dixie Valley earthquakes.

Other large magnitude Pleistocene and Holocene earthquakes identified in the area include The Gap event (3.7- 2.2 ka), an older Holocene event (age not constrained), the West Stillwater event (<5.6 ka), and another late Pleistocene event (~12-34 ka). Based on the age relationships between the spring deposits and local paleoseismic events, we suggest that: 1) the 2.0 or 3.4 ka sinter may have initiated with The Gap event; 2) the "modern" geyserite may be associated with either the 1915,  $M_s = 7.7$  Pleasant Valley, or the 1954,  $M_s = 6.8$  Dixie Valley earthquakes; and 3) that warm spring activity at about 5 ka may be associated with the M7 earthquake on the west side of the Stillwater Range. The maximum possible age for geothermal waters of the Dixie Valley system is estimated to be 12-14 ka, hence these warm and hot spring deposits represent surficial discharges of the modern geothermal system. This portion of the Dixie Valley fault, just a few kms southwest of the producing geothermal field, has actively discharged geothermal fluids in the past few thousand years, up into modern times.

### **INTRODUCTION AND GEOLOGIC SETTING**

The Dixie Valley geothermal reservoir is associated with an active normal fault, the Dixie Valley (or Stillwater) fault that occurs along the eastern margin of the Stillwater Range. In the geothermal field, the high-temperature (240° C) fluids produced from the fault zone at depths of 2-3 km power a 62 MW electrical plant operated by the Caithness Energy Corp. Active fumaroles are present along the surface trace of the Dixie Valley fault at the northern and southern ends of the geothermal field (Fig. 1). The Senator Fumaroles occur near the northern margin of the production area and smaller fumaroles (informally called the Section 10/15 fumaroles; Blackwell et al., 2000a) are active along the range front south of the geothermal field where fossil

travertine and sinter deposits are also present. These travertine and sinter deposits occur at the northern endpoint of surface ruptures along the Dixie Valley fault that are Holocene in age (Fig. 2; Caskey et al., 1996; 2000). In this paper we describe the mineralogy, occurrence, age and paleoseismic significance of these spring deposits. Future work will include the study of smaller sinter deposits in this area that have yet to be mapped or dated, including fossil sinter deposits at the nearby Dixie Comstock gold mine that Vikre (1994) suggested were related to the Dixie Valley geothermal system.

The Section 10/15 fumarole and sinter area occurs as part of the DVPP (Dixie Valley Power Partners, including ESI and Caithness Corp.) geothermal lease where two deep exploration wells (62A-23 and 36-14) were drilled in 1993 and 1994, south of the (then) Oxbow field (see Fig. 1). The sinter area is important because: 1) well 36-14 is the hottest well drilled in the entire Great Basin (with temperatures of 280 °C at about 3050 m; Benoit, 1994; Blackwell et al., 2000a; 2000b); 2) compared to a single, major fault in the current production area, the fault zone in the DVPP lease block appears to be composed of multiple faults, both inboard and outboard of the main rangefront fault (Smith et al., 2001); and 3) wells along this portion of the fault zone have variable permeabilities, well 62-23 appears to be tight (Blackwell et al., 2000a) while fluid production from well 36-14 is capable of supporting 3.5 MW (S. Petty, pers. comm.). Although the fault structure complicates development drilling, there is significant potential for further geothermal exploration and development (Robertson-Tait et al., 2000).

The local stress regime based on borehole studies in well 66-21 (Hickman et al., 1997; Barton et al., 1998), and paleoseismic studies of the Dixie Valley fault (Bell and Katzer, 1990; Caskey et al., 1996; 2000a; Caskey and Wesnousky, 2000b) has been well documented. The Hickman and Barton studies indicate that present-day fluid pressures in well 66-21 (Fig. 1) are artesian compared with subhydrostatic pressures in the main geothermal reservoir, and that faults near this well are not critically stressed for frictional failure. Even though the faults and fractures in well 66-21 were found to be optimally oriented for normal faulting, a high ratio of  $S_{\text{hmin}}$  to  $S_v$  appears to have a great effect on the fracture permeability in this nonproductive well.

The Dixie Valley geothermal field occurs in an area known as the “Stillwater seismic gap”, a 45 km-long section of the Dixie Valley fault that lies between the 1915 ( $M_s$  7.7) Pleasant Valley and 1954 ( $M_s$  6.8) Dixie Valley fault rupture zones to the north and south, respectively (Fig. 2). Recent paleoseismic

studies have provided new constraints on the timing and distributions of large magnitude late Pleistocene and Holocene earthquakes in area including: 1) The Gap event (3.7-2.2 ka) (Caskey, unpub. data) which broke along the section of the Stillwater seismic gap lying south of the geothermal field and overlapped with the 1954 rupture zone by about 20 km; 2) an older (?) Holocene event (age not constrained) that broke along the section of the Stillwater gap lying north of the geothermal field (Caskey and Wesnousky, 2000); 3) the West Stillwater event (<5.6 ka but older than The Gap event) which broke along a ~40 km section of the West Stillwater fault on the west side of the Stillwater Range (Caskey, unpub. data); and 4) a paleoseismic event (~12-34 ka) that broke in the area of the 1954 earthquake (Bell and Katzer, 1990). The Gap event produced vertical displacements of up to 5 m along the Dixie Valley fault. Surface ruptures of this event can be traced to about 10 km south of the geothermal field. A total rupture length of 45 km together with an average slip for the event of 2 to 4 m (Caskey, unpub. data) equate to an estimated moment magnitude of 7.1 to 7.3 for The Gap event. Similarly, the measured length of rupture associated with the West Stillwater event and vertical surface displacements on the order of 1-3 m indicate that these ruptures are associated with an  $M$ -7 earthquake. Ruptures for this event essentially overlap with the 1954 rupture trace on the east side of the range.

## METHODS

Preliminary mapping of the sinter and travertine deposits and sampling was done in the spring of 2001. The mineralogy of the spring deposits was determined by X-ray powder diffraction (XRD) analysis, which was especially important in understanding the crystallinity of the silica phases and tracking the progressive transformation from amorphous opal (opal-A) through opal-CT to cristobalite (opal-C) and microcrystalline quartz (nomenclature of Smith, 1998; sinter maturation model of Herdianita et al., 2000a). Petrographic and scanning electron microscopy (SEM) analyses were used to document the morphological and textural changes that accompany these mineralogical transformations. Selected samples of the spring deposits were submitted to the New Zealand Institute of Geological and Nuclear Sciences and the Rafter Radiocarbon Laboratory for detailed palynology and carbon-14 dating by Accelerator Mass Spectrometry (AMS). The  $^{14}\text{C}$  dates were then compared to known ages of paleoseismic events in the area in order to determine the temporal relationships between earthquake and spring activity along the Dixie Valley fault.

## **DESCRIPTION OF THE SPRING DEPOSITS**

In this study, a variety of spring deposits were mapped and sampled. These included two travertines, two sinter deposits and two opal-cemented alluvial or lacustrine beach gravels. Of these, four were dated using AMS spectrometry. The occurrence and mineralogy of the travertine samples is briefly described below. The sinter deposits are located in township T24N and R36E and are named by section in which they occur. They will be discussed in order of their age, with the youngest first.

### **Cottonwood Canyon Travertine**

This is a large travertine deposit approximately 1.5 km from the mouth of Cottonwood Canyon in the Stillwater Range (see Fig. 1). In most places, it is a porous travertine with abundant plant molds, and thinly-bedded where it drapes over older landslide and colluvial material, dipping steeply toward Cottonwood Creek. It occurs at the intersection of a northeast-striking normal fault (the most inboard of a set of five range front faults) and a set of north-striking vertical faults (Plank, 1999). A north-trending vertical fault cuts the travertine and here the travertine is recrystallized to a dense, sugary-textured limestone. XRD analyses of both the dense and porous varieties indicate that the travertine deposit is composed entirely of calcite. The travertine is up to 40 m thick. Efforts were made to collect an older portion of the travertine where it is cut by the vertical fault. However, the  $^{14}\text{C}$  date for the plant debris extracted from this sample returned with an age of 312 +/- 60 years BP (before present). This age likely represents younger pollen and fungal spores rather than the true age of the travertine. This travertine will be resampled during the next field campaign.

### **Section 11 Altered Area Travertine**

An area of fault intersections and altered, bleached white, pink and yellow rock occurs between two landslides at the southern margin of the geothermal field (see Alteration Zone in Section 11, Fig. 1). It is informally referred to as the "Altered Area" and is characterized by active (weak) fumarolic activity along the range front fault (Fig. 3) and the presence of advanced argillic alteration minerals (kaolin with traces of alunite). Mantling the light-colored altered rock is a travertine deposit with an unusual mineralogy. Although predominately composed of calcite (70 to 80 wt % by XRD), it also contains variable amounts of dolomite (up to 10 wt %), hematite, and barite (up to 12 wt % in some samples) in alternating light and dark-colored (perhaps algal-influenced) laminations that resemble zebra stripes (Fig. 3). In places, dark iron- and manganese-rich material cements and coats older "dirty" sand and

other alluvial and fluvial material that contain clasts of the iron-spring material. The entire spring deposit is about 1 to 3 m thick and 75 m long where it forms a resistant rib, trending north-south and dipping about 15° into Dixie Valley. It appears to have emanated from a N-trending fault mapped by Plank (1999). This fault also forms the headwall for a large landslide along the range front and may extend into the subsurface in Dixie Valley (Smith et al., 2001). The travertine predates both the landslide that overlies it to the north, and the ongoing fumarolic activity with its associated intense argillic alteration.

Because both dolomite and barite exhibit retrograde solubilities, our interpretation is that this zebra-banded travertine was deposited in a warm spring environment, and that the spring water may have been a mixture of upwelling hot geothermal waters with cool modified-meteoric or basinal waters. The  $^{14}\text{C}$  age of this travertine is 5040 +/- 60 years BP.

### **Section 15 Geyserite**

Dipping steeply off the range front about a km south of the main Section 10/15 fumarole is a large (10m by 20m) sinter deposit that can be described as "geyserite". This form of silica is characteristic of high-temperature hot spring vents. The upper portion of the deposit consists of dense vitreous silica in botryoidal knobs (Fig. 4) that coalesce upward into round heads up to 30 cm in diameter. In cross-section, these heads appear to be stromatolitic with fibrous upward-radiating biogenic structures. Thinly laminated dense silica horizons are separated by vertical palisades of filament-like structures. SEM images show that the erect filaments appear to be organic and exhibit a carbon peak on the EDX. XRD patterns of geyserite samples exhibit a large, broad hump that is characteristic of opal-A, centered about 4.0 angstroms and extending from 16 to 31° two-theta.

The geyserite appears to have emanated at an elevation of about 1160 m from a splay of the range front fault recently mapped by Smith et al. (2001). The sinter terrace mantles the range front escarpment and dips steeply from the proximal vent area into Dixie Valley (Fig. 4). Bedding plane ripplemarks, microterraces, and flowstone point in the direction of downward flow. Abundant molds of plant material are evident along these bedding planes. At the base of the escarpment, the sinter levels out into an outflow apron that is interbedded with calcareous lacustrine or pond deposits. Plant debris extracted from the upper geyserite portion of this deposit yielded a  $^{14}\text{C}$  age of *negative* 282 +/-75 years BP, which we interpret to represent as a modern date.

An older age determination for this sinter ("dense clear cryptocrystalline silica from a siliceous sinter

hot spring deposit in section 15, T24N, R36E”) was obtained by Waibel (1987) using the ionium/thorium method. The estimated age of the deposit using this method was 9,000 +/- 2,000 years.

#### Section 11 Reddish Sinter

A small siliceous sinter terrace occurs near the southernmost landslide of the altered area. It is finely laminated with pores between the laminations and is pink to red in color (Fig. 5). XRD analysis indicates that it is composed of opal-CT (85 wt %) with some quartz (11 wt %) and traces of goethite, calcite, chlorite and gypsum. In thin-section, the quartz appears to be present as clasts of older sinter deposits that became incorporated into the younger sinter.

A variety of intricate textures can be observed in thin-section. Vertical filaments (“palisades”) of silicified microbial remains appear to be present in some laminations. Wavy laminations consist of dense botryoidal opal that is completely isotropic under crossed nichols, indicating the presence of amorphous opal (opal-A). Curved laminae with lenticular voids may represent bubble mats formed during sinter deposition. Some laminations contain abundant plant or woody debris encased in opal. Most of the original plant debris has been leached away, leaving molds and casts of the delicate cellular structure. Dark clots or peloids are also present. SEM images illustrate the encrusting habit of the opal and the presence of goethite and authigenic chlorite.

In contrast to the XRD sample, most of the opal observed with the SEM appears to be dominantly opal-A although some of the surfaces exhibit small crystallites that may represent paracrystalline opal-CT (Fig. 5). No lepispheres of bladed cristobalite (opal-C or opal-CT) were observed. It is likely that this sinter is predominantly opal-CT, or opal-A transitional to opal-CT. Using XRD, an approximate measure of the structural state of a particular silica sample may be gained from the width of the ~4-angstrom diffraction line, or band, at half maximum intensity (the “FWHM” of Smith, 1998; Herdianite et al., 2000a). The width of the 4.1-angstrom peak at half maximum intensity is about 1° two-theta which suggests that the silica phase is opal-CT, rather than opal-A or opal-C. The band width of the entire peak is about 4° two-theta (from 10 to 24 two-theta) and there is a 2.5-angstrom opal-CT peak in the X-ray pattern.

Very little pollen was observed in this sample, but the abundant organic debris was dated at 2178 +/- 55 BP.

#### Section 15 Opal-cemented Gravels

Cemented gravel near the base of the Section 15 geyserite contains abundant clastic debris with a muddy matrix cemented by opal and calcite. The upper surface of this deposit is opal-cemented and flat-lying at an elevation of about 1135 m. Thin-sections show abundant unsorted, angular to subangular sand grains composed of quartz, feldspar, biotite, hornblende, and magnetite, and larger granules of diorite and silicified volcanic rock fragments, the carbonate and opal cements, and some woody plant debris. Palynologic analysis of the sample indicates abundant pollen and spore material. Colonies of the freshwater algae *Botryococcus* were found, indicating that the environment of deposition was clearly a small, warm, shallow lake or pond. The light specific gravity organic material in this sample provided a <sup>14</sup>C age of 3438 +/- 80 BP.

#### Section 10 Sinter Terraces

This deposit occurs in the canyon just north of the Section 10/15 Fumarole. It is a complex deposit consisting of calcite, hematite, quartz and opaline silica that appears to represent several hot spring episodes. These spring deposits appear to have emanated from the same range front fault as the Section 15 geyserite. Three layers of siliceous sinter occur interbedded with range front stream cobbles at elevations between 1130 and 1165 m. The lowest layer of siliceous material is only a few centimeters thick, and is mostly composed of microcrystalline quartz (Fig. 6). It appears to represent the oldest hot spring deposit in the Section 10/15 sinter area. A second terrace of siliceous sinter forms the resistant cap of an arcuate ridge of cemented alluvium and lacustrine material at an elevation of about 1135 m. This opal-cemented gravel terrace likely represents a portion of the same deposit as the Section 15 gravels (dated at 3.4 ka). The uppermost sinter terrace at an elevation of 1165 m is composed of clear opaline geyserite and appears to be identical to the modern-age Section 15 geyserite.

XRD analysis indicates that the lowest (oldest) sinter is composed of quartz (34 wt %), opal-CT (18 wt %), hematite (10 wt %), and some amorphous material (likely opal-A). Two samples were analyzed by SEM-EDX. One sample consists entirely of spherules of doubly terminated quartz crystals that clearly formed from the maturation of juvenile botryoidal opal (Fig. 6). The other sample consists of dense botryoidal opal with encrustations of hematite.

This sinter deposit was not radiometrically dated because of the variable mineralogy and potential problems with distinguishing separate spring episodes. However, based on stratigraphic relations and the abundance of prismatic quartz, some of this hot spring deposit must be older than 3.4 ka (but probably younger than Lake Dixie deposits at 11-12 ka; Caskey et al., 2000; Bell and Katzer, 1987).

### **SINTER AGING AND MINERALOGY**

The results of this study indicate that the mineralogy of the Dixie Valley sinters is clearly related to their age. In general, the modern deposits are characterized by opal-A (Fig. 4), sinter deposits that are composed of paracrystalline opal-CT are 2000 to 3500 years old (Fig. 5), and sinter deposits that contain microcrystalline quartz (Fig. 6) are between 3500 and 12,000 years old. In general, these ages are consistent with the results of sinter aging studies by Herdianita et al. (2000b). Their study showed that the transformation from juvenile noncrystalline opal to microcrystalline quartz in sinter deposits usually occurs between 10,000 and 50,000 years of age.

In New Zealand, the characterization of sinters has been used to evaluate a number of geothermal areas where sinter deposits are preserved, but very few studies have been conducted in the western U.S. (with the exception of White's pioneering work on the Steamboat Springs, Nevada and Yellowstone sinters; White et al., 1988). Although we did not use very sophisticated techniques (such as differential thermal or thermogravimetric analyses and Raman spectroscopy), the results of this study at Dixie Valley suggest that standard X-ray powder diffraction techniques can be used as a general guide to track changes in the mineralogy of the sinters and to estimate their age. Differences between the findings of this study and sinters studied in New Zealand include the apparently rapid transformation to quartz (within 12,000 years), and an absence of a strong tridymite diffraction peak in opal-CT samples from Dixie Valley and/or a rapid transformation from opal-A to quartz. At Dixie Valley, the accelerated aging may be attributed to the presence of admixed plant, clay and carbonate material (a process originally described for Beowawe, Nevada sinters by Rimstidt and Cole, 1983) and the continued high temperatures and fumarolic activity at the sinter locality, as compared for example, to the Umukuri or Te Kopia silica sinters in New Zealand where fault-related uplift has frozen the sinters in the initial stages of silica diagenesis (Herdianita, 2000b; Martin et al., 2000).

### **SUMMARY**

The maximum age of the travertines and sinters generally corresponds to the estimated age of the

fluids from the Dixie Valley geothermal field (about 12 to 14 ka) based on chemical and isotopic analyses (Nimz et al., 1999). These thermal spring deposits likely represent discharges related to the modern geothermal system. The apparent periodicity of the ages (with a recurrence interval of about 1000 to 2000 years) suggest that these discharges were episodic in nature, and also that the chemistry and the temperature of the spring waters changed between the time of deposition of the hematite and barite-bearing calcic travertine (at 5.1 ka), and the formation of the 3.4 ka and younger silica sinters. The presence of silica sinter indicates that subsurface temperatures were in excess of 175° C (Fournier and Rowe, 1966) and that the sinters formed at the ground surface from alkali chloride waters of near-neutral pH (Herdianita et al., 2000b). Fumarolic activity and acid alteration of surrounding footwall rocks apparently occurred with the intermittent lowering of the water table between times of spring flow. The duration of spring activity compared with fumarole activity is not known. However, historic records indicate that increases in spring discharges in the IXL Canyon area continued for months to several years following the 1954 Dixie Valley earthquake (Bell and Katzer, 1987).

We speculate that episodes of spring outflow along the Dixie Valley fault may correlate to local seismic events based on similarity of ages (Fig. 7). We suggest that: 1) outflow during the 3.4 ka and possibly the 2.0 ka sinters may have been initiated by stress and hydrologic changes associated with The Gap event; 2) the "modern" geysers may be associated with either the 1915 Pleasant Valley or the 1954 Dixie Valley earthquakes; and 3) the formation of the calcite-hematite-barite warm spring deposits at about 5 ka may be associated with the M7 earthquake on the west side of the Stillwater Range. Quartz-rich sinter may possibly be related to the oldest surface-rupturing event recognized along the Dixie Valley fault, bracketed between 12 ka and 35.4 ka.

### **Acknowledgements**

Funding for this project was provided under DOE contracts DE-PS07-98ID13589 (for S.J. Lutz) and DE-FG07-98ID113620 (for S.J. Caskey). The authors would like to thank the staff and management of Caithness-Dixie Valley for their logistical assistance during fieldwork sessions. Thanks also to Barb Marin of Terra Tek for the excellent SEM-EDX analyses and imagery.

### **REFERENCES:**

Barton, C.A., Hickman, S., Morin, R., Zoback, M.D., and D. Benoit, 1998, Reservoir-scale fracture permeability in the Dixie Valley, Nevada, geothermal field: Proceedings, Twenty-third Workshop on Geothermal Reservoir Engineering, Stanford University, p. 299-306.

- Bell, J.W. and Katzer, T., 1987, Surficial geology, hydrology, and late Quaternary tectonics of the IXL Canyon area, Nevada as related to the 1954 Dixie Valley earthquake: Nevada Bureau of Mines and Geology, Bulletin 102, 52p.
- Bell, J.W. and Katzer, T., 1990, Timing of late Quaternary faulting in the 1954 Dixie Valley earthquake area, central Nevada: *Geology*, v. 18, p. 622-625.
- Benoit, D., 1994, Review of geothermal power generation projects in the Basin and Range Province 1993: GRC Bulletin, May, p. 173-178.
- Blackwell, D.D., Golan, B., and Benoit, D., 2000a, Thermal regime in the Dixie Valley geothermal system: Proceedings World Geothermal Congress, Kyushu-Rohoku, Japan, May 28-June 10, 2000, p. 991-996.
- Blackwell, D.D., Golan, B., and Benoit, D., 2000b, Temperatures in the Dixie Valley, Nevada geothermal system: *Geothermal Resources Council Transactions*, v. 24, p. 223-228.
- Campbell, K.A., Rodgers, K.A., Brotheridge, J.M.A., and P.R.L. Browne, 2001, An unusual modern silica-carbonate sinter from Pavlova Spring, Ngatamariki, New Zealand: manuscript, Auckland Sinter Programme, Department of Geology- University of Auckland.
- Caskey, S.J., Wesnousky, S.G., Zhang, P., and D.B. Slemmons, 1996, Surface faulting of the 1954 Fairview Peak (Ms7.2) and Dixie Valley (Ms6.9) earthquakes, central Nevada, *Bulletin of the Seismological Society of America*, v. 86, n. 3, p. 761-787.
- Caskey, S.J., Bell, J.W., D.B. Slemmons, and A.R. Ramelli, 2000a, Historical surface faulting and paleoseismology of the central Nevada seismic belt: *Geological Society of America, Field Guide 2*, p. 23-44.
- Caskey, S.J., and S.G. Wesnousky, 2000b, Active faulting and stress redistribution in the Dixie Valley, Beowawe, and Brady's geothermal fields: implications for geothermal exploration in the Basin and Range: Proceedings, Twenty-fifth Workshop on Geothermal Reservoir Engineering, Stanford Geothermal Workshop, Stanford University, 16p.
- Fournier, R.O., and Rowe, J.J., 1966, Estimation of underground temperatures from the silica content of water from hot springs and wet-steam wells: *American Journal of Science*, v. 264, p. 685-697.
- Herdianita, N.R., Rodgers, K.A., and P.R.L. Browne, 2000a, Routine instrumental procedures to characterize the mineralogy of modern and ancient sinters: *Geothermics*, v. 29, p. 65-81.
- Herdianita, N.R., Browne, P.R.L., Rodgers, K.A., and K.A. Campbell, 2000b, Mineralogical and morphological changes accompanying ageing of siliceous sinter: *Mineralium Deposita*, v. 35, n. 1, p. 48-62.
- Hickman, S., and Zoback, M., 1998, Tectonic controls on fracture permeability in a geothermal reservoir at Dixie Valley, Nevada: Proceedings. Twenty-third Workshop on Geothermal Reservoir Engineering, Stanford University, January 26-28, 1998, p. 291-298.
- Martin, R., Mildenhall, D.C., Browne, P.R.L., and Rodgers, K.A., 2000, The age and significance of in-situ sinter at the Te Kopia thermal area, Taupo Volcanic Zone, New Zealand: *Geothermics*, v. 29, p. 367-375.
- Nimz, G., Janik, C., Goff, F. Dunlap, C., Huebner, M., Counce, D., and S.D. Johnson, 1999, Regional hydrology of the Dixie Valley geothermal field, Nevada: preliminary interpretations of chemical and isotopic data: *Geothermal Resources Council Transactions*, v. 23, p. 333-338.
- Plank, G.L., 1999, Structure, stratigraphy, and tectonics of a part of the Stillwater Escarpment and implications for the Dixie Valley geothermal system: M.S. thesis draft, University of Nevada- Reno, 153p.
- Rimstidt, J.D., and Cole, D.R., 1983, Geothermal mineralization I: the mechanism of formation of the Beowawe, Nevada, siliceous sinter deposit: *American Journal of Science*, v. 283, p. 861-875.
- Robertson-Tait, A., and J.W. Lovekin, 2000, Potential sites and experiments for enhanced geothermal systems in the western United States: *GRC Transactions*, v. 24, p. 169-174.
- Smith, D.K., 1998, Opal, cristobalite, and tridymite: noncrystallinity versus crystallinity, nomenclature of the silica minerals and bibliography: *Powder Diffraction*, v. 13, n. 1, p. 2-19.
- Smith, R.P., Wisian, K.W., and D.D. Blackwell, 2001, Geologic and geophysical evidence for intra-basinal and footwall faulting at Dixie Valley, Nevada: *Geothermal Resources Council Transactions*, v. 25, p. 323-326.

Vikre, P.C., 1994, Gold mineralization and fault evolution at the Dixie Comstock Mine, Churchill County, Nevada: *Economic Geology*, v. 89, n. 4, p. 707-719.

Weibel, A.F., 1987, An overview of the geology and secondary mineralogy of the high temperature geothermal system in Dixie Valley, Nevada:

*Geothermal Resources Council Bulletin*, v. 16, n. 9, p. 5-11.

White, D.E., Hutchinson, R.A., and T.E.C. Keith, 1988, The geology and remarkable thermal activity of Norris Geyser Basin, Yellowstone National Park, Wyoming: United States Geological Survey Professional Paper 1456, p. 1-84

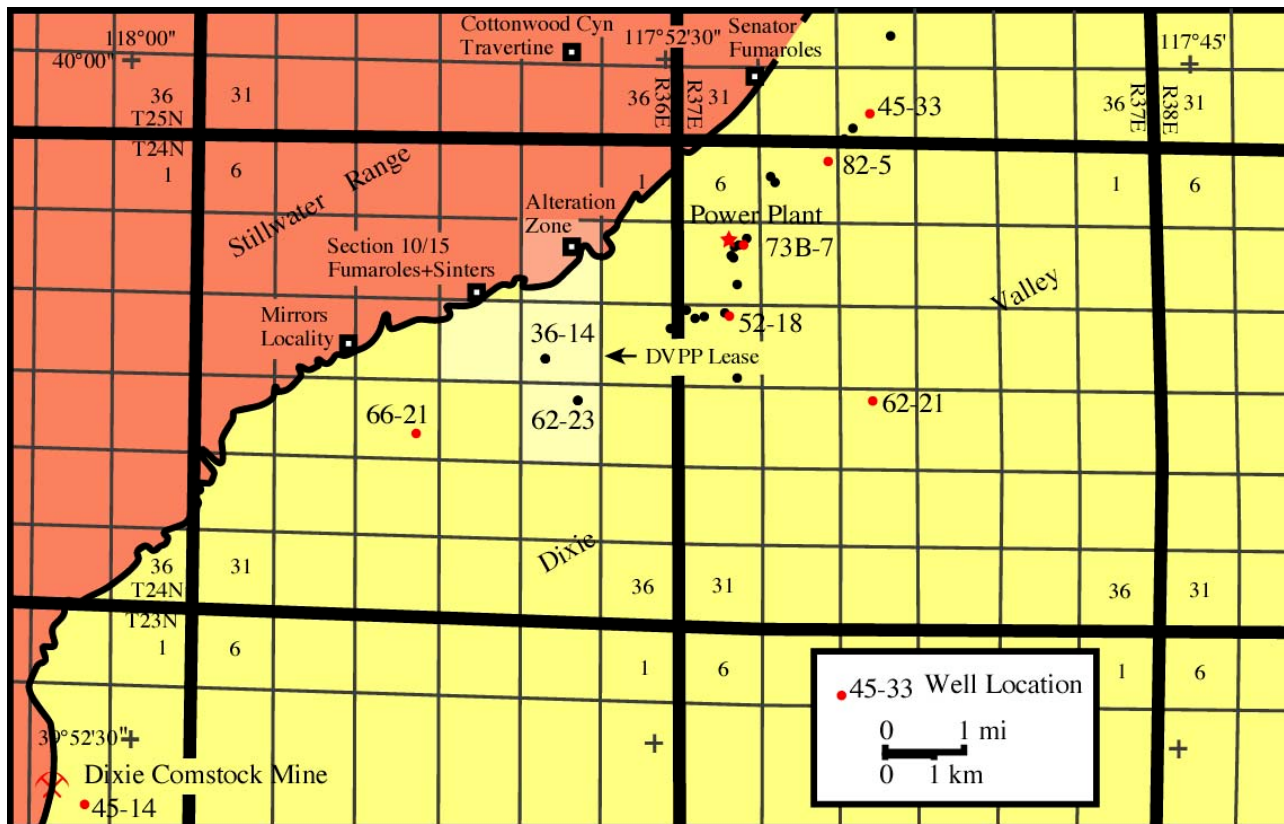


Fig. 1. Location of selected wells in the Dixie Valley geothermal field, and travertine and sinter sample localities along the Stillwater range front in northern Dixie Valley, Nevada. Hot spring sinter deposits occur along the surface trace of the Dixie Valley fault in Sections 10, 11 and 15 of R36E T24N.

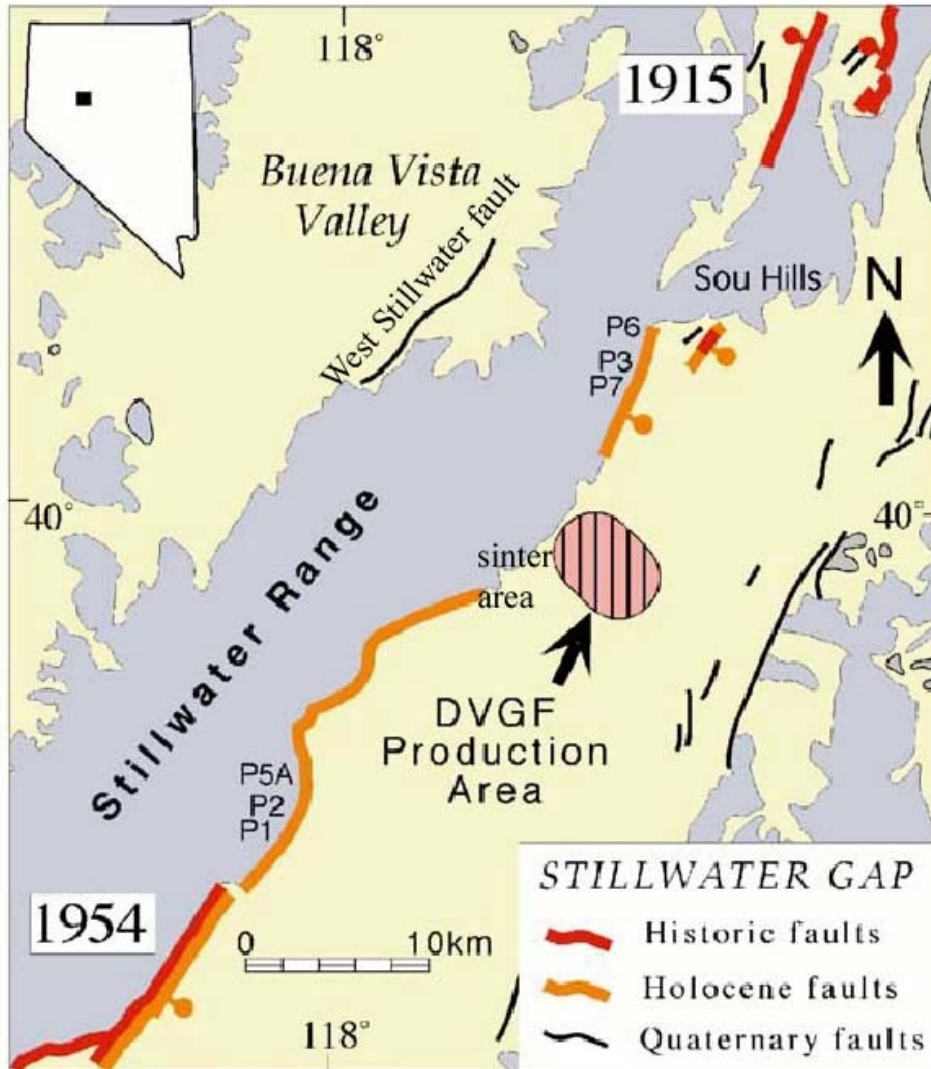


Fig. 2. Generalized fault map of the Stillwater Gap area showing the distribution of the historic 1915 M7.7 Pleasant Valley and 1954 M6.8 Dixie Valley fault ruptures (bold red lines), Holocene ruptures (bold orange lines) and Quaternary faults (thin black lines). The Dixie Valley geothermal field (DVGF) occurs in an area where recent fault scarps are not recognized. Fossil hot spring sinters occur at the northern endpoint of surface ruptures that are Holocene in age, just south of the Dixie Valley production area.



Fig. 3. Alternating light (calcite and dolomite) and dark (hematite) laminations in Section 11 travertine. This fossil warm spring deposit forms a terrace that mantles light-colored, argillically-altered rocks at the "Altered Area". It occurs along a north-trending fault and appears to predate both the argillic alteration and ongoing weak fumarolic activity, and a landslide that overlies it to the north. Organic debris in the travertine was dated at ~5040 years before present.

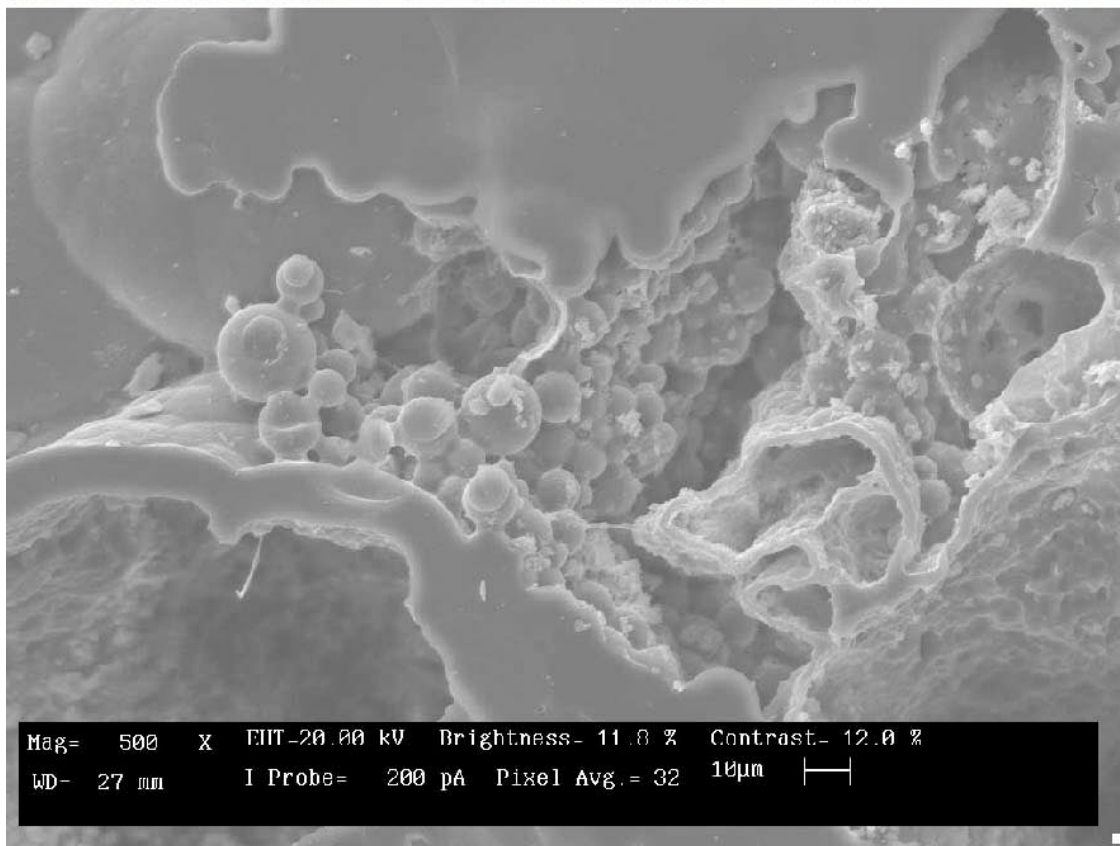


Fig. 4. The Section 15 sinter is composed of steeply-dipping "geyserite" proximal to the hot spring vent (see light-colored area to the right of the person), and a flat-lying outflow apron (in foreground). The SEM image illustrates opal-A spherules, dense vitreous opal, and a few organic filaments. This sinter has a modern radiocarbon age.

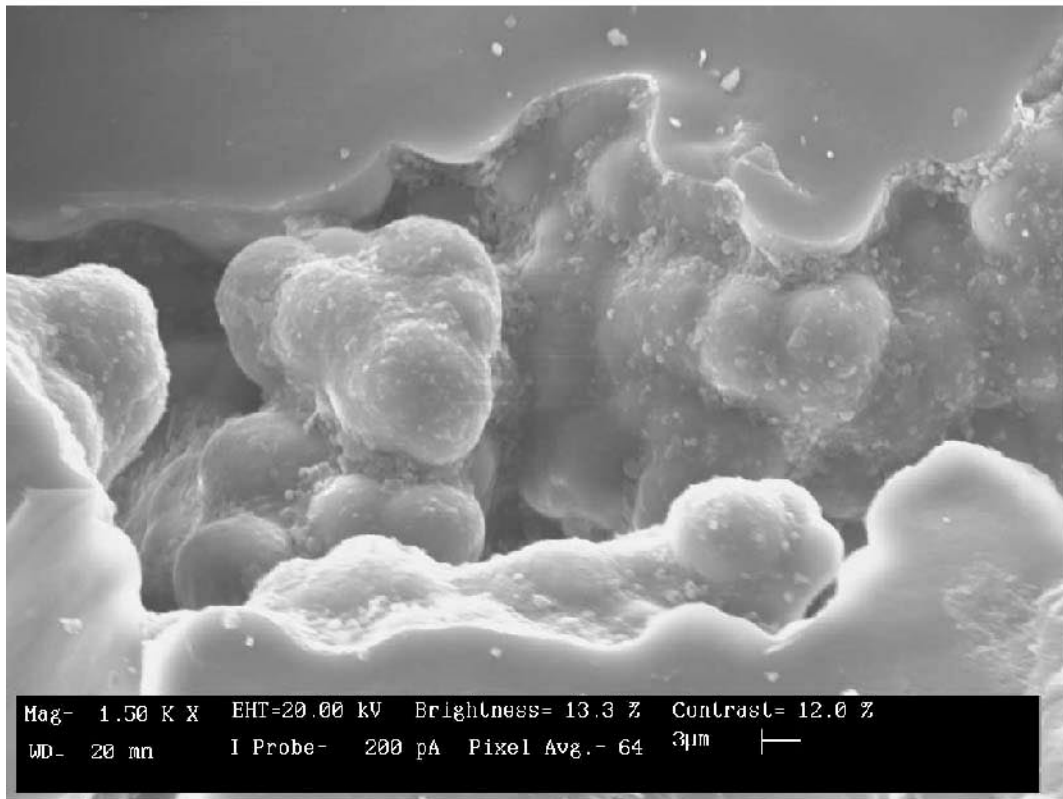


Fig. 5. The Section 11 sinter dips gently towards Dixie Valley. It is composed of opal-A transitional to opal-CT (see text). The SEM image displays this transitional morphology; the botryoidal opal has slightly recrystallized from the originally smooth opal-A, but does not display the typical bladed texture of cristobalite. Organic material in this sinter was dated at ~2178 years before present.

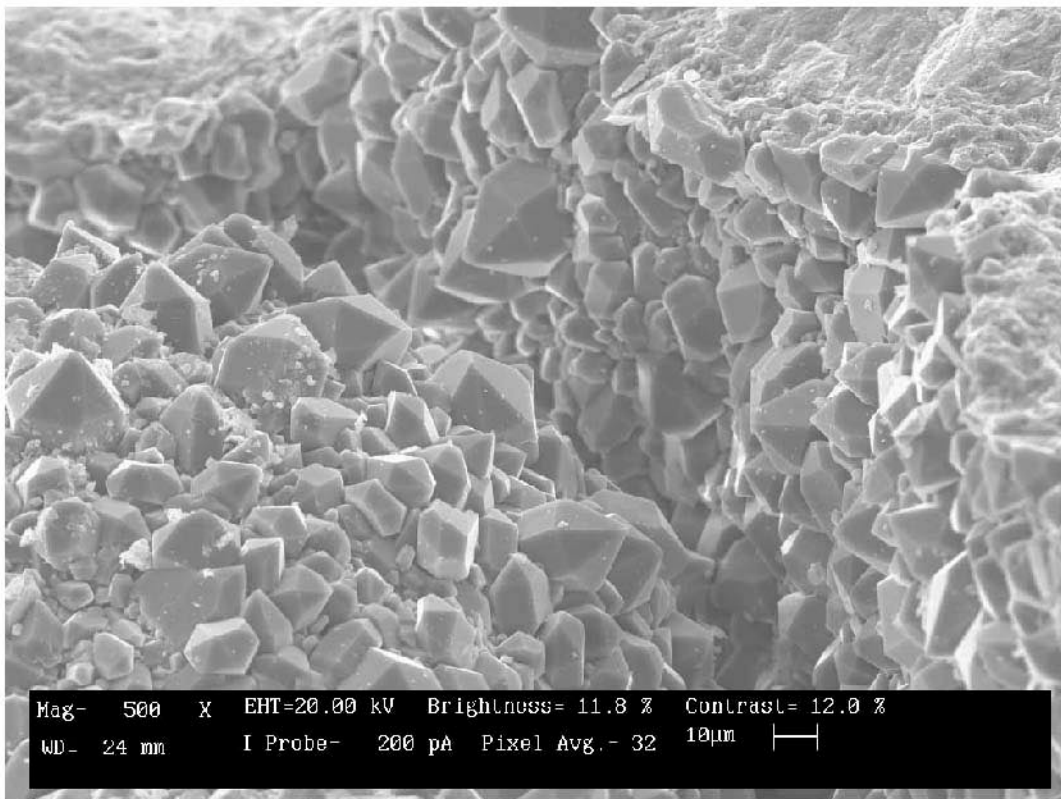


Fig. 6. The oldest of three sinter terraces in the Section 10 area is composed of prismatic quartz that clearly formed from the maturation of juvenile botryoidal opal (see SEM image). This sinter terrace is only a few cms thick and is overlain by about 35 m of cemented alluvial and fluvial deposits and younger sinter deposits. The quartz-rich sample was not radiometrically dated but is estimated to be older than 3.4 ka and younger than 12 ka.

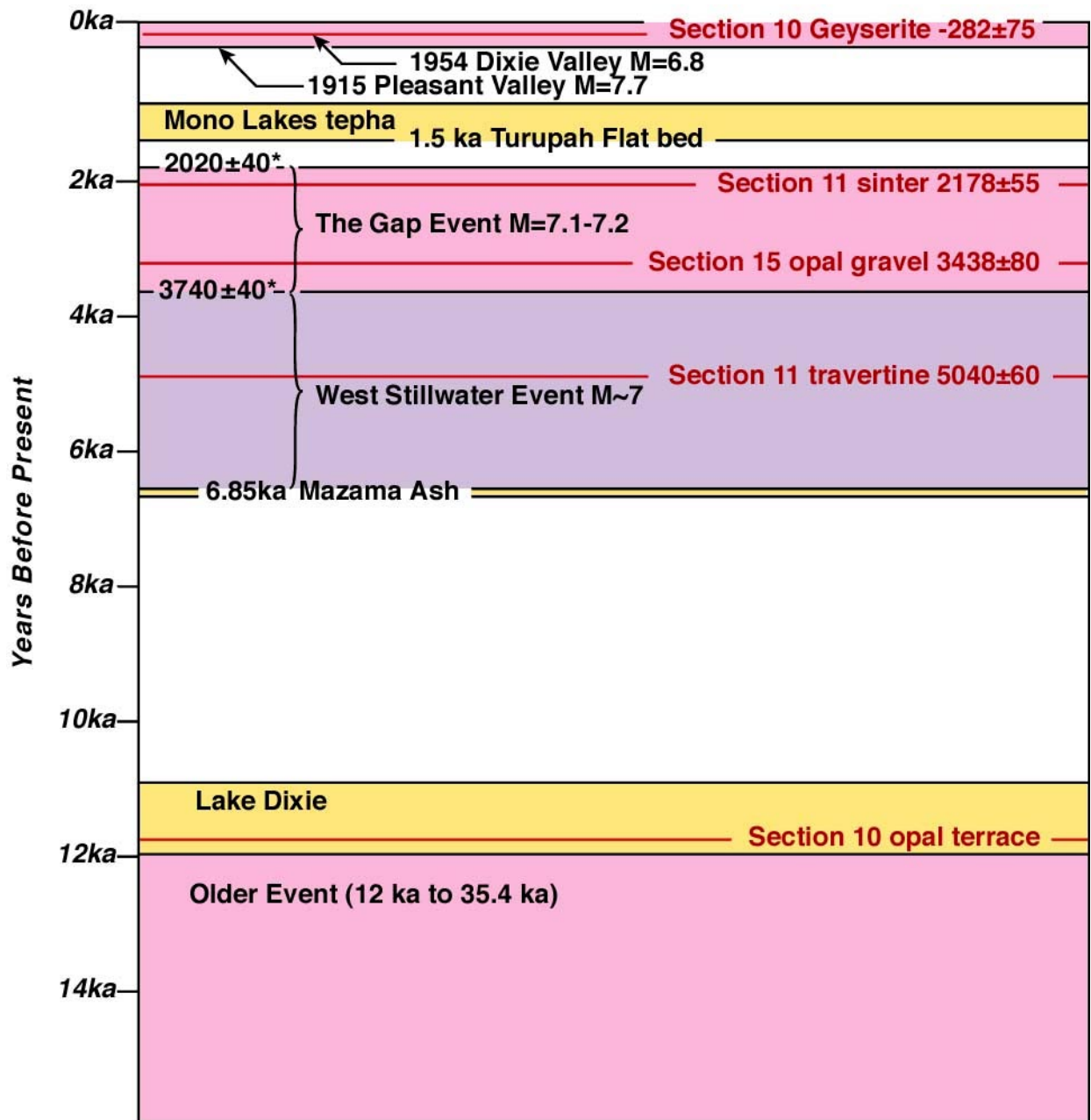


Fig. 7. Summary chart with ages of local tephas and pluvial lakes (yellow), and bracketed ages of known historic and paleoseismic surface-rupturing fault events in the northern Dixie Valley area (pink and purple) on the left, to compare with radiocarbon dates for the study sinter and travertine deposits (right side of diagram). Bracketed age of The Gap event from  $^{14}\text{C}$  dating of carbonaceous sediment in study trench located near the Dixie Comstock mine. The age of the Section 10 opal terrace is not constrained (maximum age indicated on chart).